Density-functional based tight-binding study of small gold clusters

P Koskinen[1,2]**, H Häkkinen**[2]**, G Seifert**[3]**, S Sanna**[4]**,
Th Frauenheim**[4] **and M Moseler**[1,5]

[1] Fraunhofer-Institut für Werkstoffmechanik IWM, Wöhlerstr 11,
79108 Freiburg, Germany
[2] Department of Physics, NanoScience Center, 40014 University of Jyväskylä,
Finland
[3] Institut für Physikalische Chemie, TU Dresden, Mommsenstrasse 13,
01062 Dresden, Germany
[4] Department Physik, Fakultät für Naturwissenschaften, Universität Paderborn,
33095 Paderborn, Germany
E-mail: michael.moseler@iwm.fraunhofer.de

Abstract. In this paper, we report the ability of self-consistent-charge density-functional based tight-binding method to describe small gold clusters. We concentrate our investigations mainly on anions, and find that the method describes their geometric and electronic structures fairly well, in comparison with density-functional calculations. In particular, the method correctly reproduces the planarity of ground-state structures up to cluster sizes in agreement with experiment and density-functional theory.

[5] Author to whom any correspondence should be addressed.

Institute *of* **Physics** Φ DEUTSCHE PHYSIKALISCHE GESELLSCHAFT

Contents

1. Introduction

Gold nanostructures and gold-based complexes are currently under active investigations in various areas of nanoscience and nanotechnology due to some remarkable physical and chemical properties of gold that appear only in the nanometer scale and/or in reduced dimensions [1, 2]. For example, gold has been shown to exhibit surprising mechanical properties in nanoscale by forming stable nanowires and nanobridges with quantized electrical conductivity, which has great relevance in understanding atomic junctions [3]. Optical absorption by gold nanoparticles depend sensitively on the size, and this property can be used e.g. in labelling applications or in devising precision therapy for selective imaging and destruction of cancer cells [4]. While totally inert as bulk phase, gold clusters and nanoparticles can be surprisingly active catalysts for oxidation and hydrogenation reactions [5]–[9]. Finally, anomalously strong relativistic bonding effects stabilize cluster structures that are unexpected and qualitatively different from the ones formed for clusters of the neighbouring elements in the Periodic Table [10]–[12].

Common to many of the above phenomena is the need to understand the relevant structures and their functionality on the quantum-mechanical level. Here, the method of choice has been the density-functional theory (DFT) since it has the best performance/cost ratio for systems with hundreds of valence electrons. While detailed information on the electronic structure of a given cluster, nanoparticle or nanostructure can be obtained via DFT, the practical bottleneck is often the satisfactory exploration of the complicated potential energy surface due to computational demands that would exceed the resources by several orders of magnitude. This complicates systematic searches for global energy minima and often precludes finite-temperature dynamical simulations. Therefore, development of methods that still maintain the important aspects of electronic structure (preferentially information parametrized from DFT calculations) but at the same time are many orders of magnitude more effective than standard DFT is in high demand.

In the past, extended Hückel theory (EHT) and related methods have been used for inexpensive calculations of relativistic systems [13, 14]. Often these schemes have proven to yield rather reliable semi-quantitative results. Here, we investigate systematically the applicability of the density-functional based tight-binding method [15]–[17] to describe the physics of small gold clusters. This method, although formally similar to EHT, is less empirical since it can be derived from DFT employing a controlled chain of approximations. Like EHT, it is very competitive in the above-mentioned computational performance. We concentrate on gold anions, and therefore employ always the modification of the method which takes into account the charge transfer effects within the cluster (self-consistent-charge density-functional tight-binding, SCC-DFTB; here DFTB for short). We shall demonstrate that the method works, in addition to a few non-metals (see e.g. [15, 17]) and metals (see [18]), for gold as well.

It produces the correct geometrical properties for the clusters. In particular, the tendency to two-dimensional ground states is correctly reproduced, although the isomer ordering is only in partial agreement with the corresponding ordering in DFT. In addition, cohesive energies are systematically overestimated. Electronic properties, such as electron detachment energies and densities of states the method yields in reasonable agreement with DFT.

In the following section, we briefly review the DFTB method and describe its parametrization for gold. (For a detailed description of the method, we refer to the original papers [15, 17, 19, 20].) In section 3, we compare structural and electronic properties of gold cluster anions, Au_N^-, $4 \leqslant N \leqslant 14$, calculated with the DFTB method, to the previously published Kohn–Sham DFT results [21]. Conclusions are given in section 4.

2. Method

The practice in general non-orthogonal tight-binding formalism is to solve for a generalized eigenvalue problem

$$\sum_{\nu} c_{\nu}^{i}(H_{\nu\mu} - \epsilon_i S_{\nu\mu}) = 0 \tag{1}$$

with eigenstates

$$|\Psi_i\rangle = \sum_{\nu} c_{\nu}^{i}|\varphi_{\nu}\rangle \tag{2}$$

that are expressed by means of a non-orthogonal localized atomic basis $\{|\varphi_{\nu}\rangle\}$ with overlaps of $S_{\nu\mu} = \langle\varphi_{\nu}|\varphi_{\mu}\rangle$. In the DFTB theory, the orbital part of the electronic interaction for N atoms in a given configuration $\{\mathbf{R}_{\alpha}, \alpha = 1, \ldots, N\}$ is described by a Hamiltonian that consists of a charge independent part H^0 and a Coulomb term for charge overlaps between neighbouring atoms

$$H_{\nu\mu} = H_{\nu\mu}^0 - \tfrac{1}{2}S_{\nu\mu}[\phi(\mathbf{R}_{\alpha}) + \phi(\mathbf{R}_{\beta})] \quad \forall \nu \in \alpha, \quad \mu \in \beta. \tag{3}$$

The components of the atomic Hamiltonian, in a two-centre approximation,

$$H_{\nu\mu}^0(R) = \langle\varphi_{\nu}(0)|H^0|\varphi_{\mu}(R)\rangle \tag{4}$$

for the 6s, 6p and 5d pseudo-atomic basis functions of gold are obtained by solving scalar relativistic [22] Kohn–Sham equation and are shown in figure 1. For the exchange-correlation functional the LDA approximation within the Ceperley–Alder parametrization [23] was used. A harmonic contraction potential $(r/r_0)^2$ has been added as introduced by Eschrig [24, 25] to form a more efficient basis set for molecular and solid state systems. The parameter r_0 is chosen to be about two times the atomic radius [26]. The atomic orbitals can be represented by linear combinations of Slater-type orbitals (STO)

$$\varphi_{\mu}(\mathbf{r}) = \sum_{\zeta}\sum_{i}(a_{\zeta i}r^{l+i})\,\mathrm{e}^{-\zeta r}Y_{lm}\left(\frac{\mathbf{r}}{r}\right), \tag{5}$$

where l and m are the angular momentum and the magnetic quantum numbers associated with the orbital μ, respectively. Extensive tests have shown that five different values of ζ and $i = 0, 1, 2, 3$ form a sufficiently accurate basis set [24].
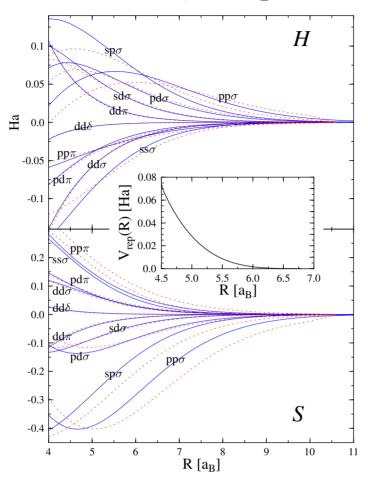
Figure 1. The Hamiltonian (upper panel) and overlap (lower panel) Slater–Koster matrix elements from scalar-relativistic (blue solid line) and non-relativistic (red dashed line) calculations. The inset shows the repulsive potential fitted to the scalar-relativistic DFT total energy calculation for the gold dimer (non-relativistic repulsion is very similar). The scalar-relativistic (non-relativistic) orbital energies used in the parametrization are: $\epsilon_{6s} = -0.2149(-0.1495)$ Ha, $\epsilon_{6p} = -0.0096(-0.0037)$ Ha and $\epsilon_{5d} = -0.2537(-0.2921)$ Ha, and we used $U = 0.25$ Ha. The repulsive part (inset) depends on two parameters, $R_d = 2.54\,\text{Å}$ (DFT-GGA equilibrium bond length of Au_2) and $R_c = 3.6\,\text{Å}$ (for $V_{\text{rep}}(R_c) = V'_{\text{rep}}(R_c) = V''_{\text{rep}}(R_c) = 0$).

The second term of the Hamiltonian (3) represents the energy shifts in the single-electron matrix elements due to the Coulomb interaction with the internal (from the Mulliken charges) and possible external electrostatic potentials,

$$\phi(\mathbf{R}_\alpha) = \phi_{\text{int}}(\mathbf{R}) + \phi_{\text{ext}}(\mathbf{R}) = \sum_\beta \gamma_{\alpha\beta}(R_{\alpha\beta})(-\Delta q_\beta) + \phi_{\text{ext}}(\mathbf{R}_\alpha). \tag{6}$$

This term takes into account the charge transfer effects, and since it depends on the (excess or deficit) atomic Mulliken charges Δq_α that are calculated from the occupied eigenstates,

the problem has to be solved self-consistently. The coupling function $\gamma_{\alpha\beta}(R)$ is the measure for the interaction strength for two spherical charge distributions separated by a distance R. It behaves for large distances like $\sim 1/R$; for all distances and Gaussian shaped-charge distributions [27] it can be calculated analytically to yield

$$\gamma_{\alpha\beta}(R) = \text{erf}(C_{\alpha\beta}R)/R. \tag{7}$$

Here, $\text{erf}(x)$ is the error function,

$$C_{\alpha\beta} = 2\sqrt{\ln 2/(W_\alpha^2 + W_\beta^2)}, \tag{8}$$

and W_α is the full width at half-maximum of the Gaussian charge cloud. Since the method is not sensitive to the exact form of the charge cloud, the Gaussian shape was chosen due to its simplicity in analytical calculations. The parameter W_α is determined by the on-site interaction (the Hubbard-U) in the limit

$$U_\alpha = \lim_{R\to 0} \gamma_{\alpha\alpha}(R) = \sqrt{\frac{8\ln 2}{\pi}} W_\alpha^{-1}. \tag{9}$$

Physically U is twice the chemical hardness, and we have used the corresponding tabulated value of gold, $U = 6.80$ eV [28].

The Hamiltonian discussed above is connected to a total energy expression

$$E = \sum_i^{occ.} \langle \Psi_i|H^0|\Psi_i \rangle + \sum_{\alpha=1}^N (-\Delta q_\alpha)[\tfrac{1}{2}\phi_{\text{int}}(\mathbf{R}_\alpha) + \phi_{\text{ext}}(\mathbf{R}_\alpha)] + E_{\text{rep}}. \tag{10}$$

The last term in (10) represents the repulsion between the atomic cores, with

$$E_{\text{rep}} = \sum_{\alpha < \beta} V_{\text{rep}}(R_{\alpha\beta}), \tag{11}$$

where $V_{\text{rep}}(R)$ is a simple short-ranged function with a cut-off R_c, as shown in figure 1. In the generation of the right geometrical properties for the clusters, the qualitative shape of $V_{\text{rep}}(R)$ appears to be important even though it is only a simple function (as opposed to the much more complex band-energy part). We want to describe our fitting method of $V_{\text{rep}}(R)$ partly due to the importance of the function but partly also due to the lack of previous detailed method descriptions. In principle, the recipe to calculate $V_{\text{rep}}(R)$ is straightforward: $E_{\text{DFT}}(R)$ of gold dimer (or some other reference structure with equal nearest-neighbour distances) is calculated with various interatomic distances R, and $V_{\text{rep}}(R)$ is obtained from the equation $E_{TB}(R) = E_{\text{DFT}}(R)$. This method is quite unpractical, since it introduces discontinuities or at least some peculiarities around R_c. Instead, we prefer to use the first and second derivatives of the previous equation. Firstly, $V'_{\text{rep}}(R_d)$ and $V''_{\text{rep}}(R_d)$ are obtained from the DFT dimer equilibrium bond length R_d, curvature $E''_{\text{DFT}}(R_d)$, and from the orbital energy part of DFTB. Secondly, using this information we employ a natural cubic spline to interpolate $V'_{\text{rep}}(R)$ from R_c to R_d and beyond, and integrate from R_c backwards to get $V_{\text{rep}}(R)$. Here also the physical requirement $V'_{\text{rep}}(R_c) = 0$ is used. The cut-off itself is chosen such that it yields $V''_{\text{rep}}(R_c) \approx 0$, in this case $R_c = 3.6$ Å. This value falls conveniently between the first- and second-nearest-neighbour distances of bulk gold.

This fitting method gives a smooth and featureless function, which is important for transferability. Furthermore, without being limited by some specific functional form, one can easily add adjustable points to the spline interpolation for a controlled fine-tuning. Even though the method does not use any energetic information from the dimer and hence does not necessarily give the right dimer binding energy, we note that the discrepancy between DFTB and DFT binding energy curves begins already beyond R_c, i.e. from the orbital energy part, and cannot be altered by the short-range repulsion. Finally, we note that this fitting method is not specific to gold, and has been applied successfully also to a few other elements.

3. Comparison of DFTB and DFT

Figure 2 shows the ground states and a few of the lowest-lying cluster isomers of small gold cluster anions in the size range 4–14 as determined in a previous DFT study [21]. In order to benchmark the performance of our novel tight-binding parametrization, we use these structures as a test set. Starting from the DFT structures the anionic clusters were reoptimized using our Freiburg–Jyväskylä DFTB code. Most of the isomers are geometrically very similar in DFTB, which means that for most of the clusters quite little structural relaxation takes place when DFTB quenching is started from DFT geometries. In other words, if these structures would have been *found* with DFTB, only a small structural relaxation would have been needed to arrive at the local minima of DFT. Still some isomers may not be stable in DFTB, as is the case e.g. for Au_7^- for which the first DFT-isomer 7B relaxes to the ground-state structure 7A. The average bond lengths are consistently larger for most smaller clusters, and this is reflected in larger clusters in a way that they become slightly 'rounded' with DFTB.

Figure 3(a) displays the cohesion and vertical detachment energies (VDEs) of the clusters shown in figure 2. The energy differences have the same scale and the qualitative DFT-trends in the ordering are nicely reproduced. The ordering of isomers is not always correct, and also the DFTB-predicted ground state can be wrong. The absolute cohesive energy is consistently overestimated by $\sim 0.3\,\mathrm{eV\,atom^{-1}}$, even though the atomic spin-polarization energy is already subtracted from the DFTB cohesion energy [15]. The energy differences and the correlations in isomer ordering, as well as our preliminary calculations reflect the correct description of the whole potential energy surface, making DFTB an ideal tool for molecular dynamics simulations to study, e.g. cluster melting and other dynamical properties.

We wish to note here that for a given cluster size, the isomer ordering could be rearranged by tuning the repulsive potential, although with the price of losing the transferability for other sizes. This demands pre-existing results and is naturally not always possible.

Especially, we want to point out that the model agrees with DFT in the description of the unusual stability of planar gold clusters [10, 21, 29, 30]. This origin of the planarity was traced back to relativity [10, 31], and indeed, if we relax e.g. Au_7^- clusters (and also other clusters with $N > 7$) using non-relativistic parametrization, we obtain three-dimensional ground states. In this sense, our DFTB parametrization for gold captures the essential features of its interatomic bonding.

While we have shown that the structural properties of the clusters are reproduced surprisingly well by fitting the repulsive part only with data from Au_2, the electronic Hamiltonian displays the limitations of the method more transparently. Figure 3(b) shows the vertical electron detachment energies using the DFT structures of figure 2. The trends in the VDEs are mainly reproduced
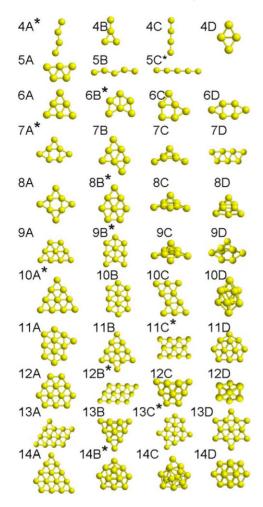
Figure 2. Clusters Au_N^-, optimized with DFT [21]. The DFT ground-state structure is labelled by A for each size[6]. The DFTB ground states are indicated by an asterisk. Note, that the DFTB ground-states show changes in dimensionality in the same size range as the DFT ground states. DFTB (DFT) shows a linear/planar transition between Au_5^- and Au_6^- (Au_4^- and Au_5^-). A planar/three-dimensional transition occurs between Au_{13}^- and Au_{14}^- for DFTB and between Au_{14}^- and Au_{15}^- in DFT. For the sake of completeness, we would like to remark that an 'A'-shaped structure has been reported by Fernandez *et al* [12] as the first higher lying isomer of Au_5^-. Within our plane wave DFT, this structure turned out to be 0.03 eV better in energy than our previous ground state 5A.

nicely, even though it appears that the absolute values are underestimated by $\sim$0.5 eV for most isomers and cluster sizes.

Even a more demanding way to test the electronic structure is to inspect the density of states (DOS). A comparison of DOS between DFTB and DFT for the ground states of $N = 8$, 10 and

---

[6] We wish to correct here a misprint in [21]: structures 13B and 13C should be interchanged in figure 4 (however, their properties are described correctly in table 1 of that paper).
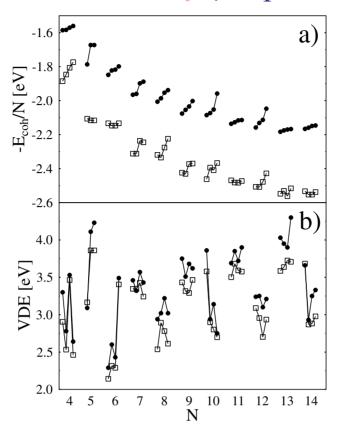
Figure 3. (a) The DFT (full circles) and DFTB (empty squares) cohesive energies (b) and VDEs for the energy-ordered (left data point corresponds to the DFT ground-state structure for each size) structures shown in figure 2. The spin-polarization energy (0.19 eV) of the neutral gold atom has been taken into account in calculating the DFTB cohesive energies. VDE is calculated in the DFT-optimized geometries and for the sake of comparison is shifted higher for every cluster by 0.5 eV.

12 can be seen in figures 4–6, respectively. The numerical efficiency of DFTB even allows for the study of thermal broadening effects of the DOS. Figure 4(c) shows the result of a 50 ps room temperature trajectory of Au_8^-. By analysing the resulting thermally averaged DOS additional dynamical information can be extracted from experiments [32].

In general, there exists a rough agreement between the DOS in different methods, such as the overall energy scale, the onset of the high DOS ('d-band') and the form of the DOS in general. The most important region is the DOS of the highest occupied states, showing the energy positions of individual states, since this is the region that can be compared to experiments. In this region one can identify similarities, such as double peaks and larger gaps. Most of the gaps in DFTB are underestimated, but often they do exist and, most importantly, can be identified. This is especially useful in the search for correct isomers e.g. if experimental photoelectron spectrum exhibits characteristic gaps [21]. Out of the three examples given here, DFTB spectra for $N = 8$, 10 (figures 4 and 5) are in a remarkable agreement with the DFT spectra. On the other hand, the agreement is not so good in some cases, as shown, e.g. for $N = 12$ in figure 6. This shows that one cannot use merely DFTB results for interpretations of experimental electronic spectral data.
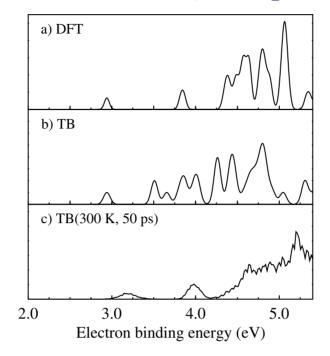
Figure 4. Density of electron states (in arbitrary units) for the ground-state structure of Au_8^- calculated with (a) DFT and (b) DFTB. Gaussian broadening of $\sigma = 0.05$ eV for the electronic eigenvalues (up- and down-spin contributions for DFT) was used, and the first peak in (a) was shifted to correspond to the VDE (i.e. $VDE = -e_{HOMO}$) in the spirit of similar procedure in DFT calculations [33, 34]. The VDE for DFTB (b) was shifted by 0.6 eV in order to match the self-consistently calculated DFT VDE value in (a) for comparison between the spectra. (c) Time-averaged DOS (without Gaussian broadening) of a DFTB molecular dynamics run for Au_8^- over 50 ps at 300 K.
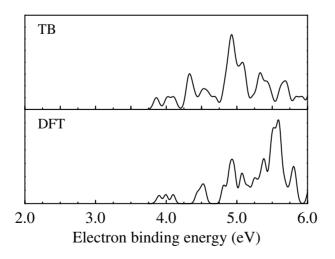

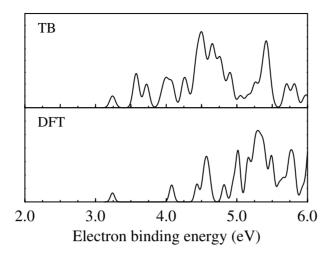**Figure 5.** Same as figure 4 for $N = 10$.

Figure 6. Same as figure 4 for $N = 12$.

4. Conclusions

We have investigated the performance of a charge-self-consistent density-functional-based tight-binding method to describe physical properties of small anionic gold clusters up to $N = 14$. We benchmarked the method against previously published DFT-GGA results [21]. The theoretical ground-state structures reported previously [21, 29] are currently understood (up to about $N = 12$) as those that also appear in cluster beam experiments at low temperatures, based on comparisons to photoelectron spectroscopy [21] and mobility data [29]. While isomer energy ordering is only qualitatively right, the geometrical properties themselves are fairly well reproduced. The VDEs follow qualitatively the trend of DFT results, and also densities of states share the same characteristic features, although not in every case. Hence the combination of the energetic information together with VDE and the DOS not only makes DFTB quite a powerful tool in the pre-selection of possible candidates for further higher level calculations, but makes DFTB results relevant also on their own right. DFTB is also a very effective tool for bonding and other electronic structure analysis of clusters and nanostructures. We remark here that e.g. the calculation of the time-averaged DOS of Au_8^- in figure 4(c) takes only a few minutes in a typical desktop computer. Note, that a comparable DFT calculation would take more than four orders of magnitude longer. Due to the conceptual simplicity and small computational cost, we expect that DFTB will be a valuable tool for the ongoing research on small gold nanostructures.

Acknowledgments

Institute *of* **Physics** ⬡ DEUTSCHE PHYSIKALISCHE GESELLSCHAFT

References

[1] See, e.g., review articles in *Gold Bull.* 2004 **37**

[2] Pyykkö P 2004 *Angew. Chem. Int. Edn. Engl.* **43** 4412

[3] Agrait N, Yeyati A L and van Ruitenbeek J M 2003 *Phys. Rep.* **377** 8103

[4] Loo C, Lowery A, Halas N, West J and Drezek R 2005 *Nano Lett.* **5** 709

[5] Haruta M 1997 *Catal. Today* **36** 153

[6] Bond G C and Thompson D T 1999 *Catal. Rev.—Sci. Eng.* **41** 319

[7] Sanchez A, Abbet S, Heiz U, Schneider W-D, Häkkinen H, Barnett R N and Landman U 1999 *J. Phys. Chem.* A **103** 9573

[8] Häkkinen H, Abbet S, Sanchez A, Heiz U and Landman U 2003 *Angew. Chem. Int. Edn. Engl.* **42** 1297

[9] Yoon B, Häkkinen H, Landman U, Wörz A, Antonietti J-M, Abbet S, Judai K and Heiz U 2005 *Science* **307** 403

[10] Häkkinen H, Moseler M and Landman U 2002 *Phys. Rev. Lett.* **89** 033401

[11] Häkkinen H, Moseler M, Kostko O, Morgner N, Hoffmann M A and von Issendorff B 2004 *Phys. Rev. Lett.* **93** 093401

[12] Fernández E M, Soler J M, Garzón I L and Balbás L C 2004 *Phys. Rev.* B **70** 165403

[13] Lohr L L and Pyykko P 1979 *Chem. Phys. Lett.* **62** 333

[14] Laarsson S and Pyykko P 1986 *Chem. Phys.* **101** 355

[15] Porezag D, Frauenheim T, Köhler T, Seifert G and Kaschner R 1995 *Phys. Rev.* B **51** 12947

[16] Seifert G, Porezag D and Frauenheim T 1996 *Int. J. Quantum Chem.* **58** 185

[17] Elstner M, Porezag D, Jungnickel G, Elstner J, Haugk M, Frauenheim T, Suhai S and Seifert G 1998 *Phys. Rev.* B **58** 7260

[18] Köhler C, Seifert G and Frauenheim T 2005 *Chem. Phys.* **309** 23

[19] Foulkes W M C and Haydock R 1988 *Phys. Rev.* B **39** 12520

[20] Frauenheim T, Weich F, Köhler T, Uhlmann S, Porezag D and Seifert G 1995 *Phys. Rev.* B **52** 11492

[21] Häkkinen H, Yoon B, Landman U, Li X, Zhai H J and Wang L-S 2003 *J. Phys. Chem.* A **107** 6168

[22] Heera V, Seifert G and Ziesche P 1984 *J. Phys. B: At. Mol. Phys.* **17** 519

[23] Ceperley D M and Alder B I 1980 *Phys. Rev. Lett.* **45** 566

[24] Eschrig H 1988 *Optimized LCAO Method and the Electronic Structure of Extended Systems* (Berlin: Akademie-Verlag)

[25] Eschrig H and Bergert I 1978 *Phys. Status Solidi* b **90** 621

[26] Frauenheim T, Seifert G, Elstner M, Hajnal Z, Jungnickel G, Porezag D, Suhai S and Scholz R 2000 *Phys. Status Solidi* b **217** 41

[27] Bernstein N 2002 *Phys. Rev.* B **66** 075212

[28] Parr R G and Yang W 1989 *Density Functional Theory of Atoms and Molecules* (New York: Oxford University Press)

[29] Furche P, Ahlrichs R, Weis P, Jacob C, Gilb S, Bierweiler T and Kappes M 2002 *J. Chem. Phys.* **117** 6982

[30] Grönbeck H and Broqvist P 2005 *Phys. Rev.* B **71** 073408

[31] Pyykkö P 1988 *Chem. Rev.* **88** 563

[32] Moseler M, Huber B, Häkkinen H, Landman U, Wrigge G, Hoffmann M A and von Issendorff B 2003 *Phys. Rev.* B **68** 165413

[33] Akola J, Manninen M, Häkkinen H, Landman U, Li X and Wang L-S 1999 *Phys. Rev.* B **60** R11297

[34] Akola A, Manninen M, Häkkinen H, Landman U, Li X and Wang L-S 2000 *Phys. Rev.* B **62** 13216